

DUAL-STEEL FRAMES FOR MULTISTORY BUILDINGS IN SEISMIC AREAS

D. Dubina***

* The "Politehnica" University of Timisoara, 1 Ioan Curea, 300224 Timisoara, Romania
e-mail: dan.dubina@ct.upt.ro

** Romanian Academy, Timisoara Branch, 24 Mihai Viteazul, 300223 Timisoara, Romania

Keywords: Dual steel, High strength steel, Ductility.

***Abstract.** Seismic resistant building frames designed as dissipative structures must allow for plastic deformations to develop in specific members, whose behavior has to be predicted by proper design. Members designed to remain elastic during earthquake, such as columns, are responsible for robustness of the structure and prevention the collapse, being characterized by high strength demands. Consequently, a framing solution obtained by combining HSS and MCS, is natural. The robustness of structures to severe seismic action is ensured by their global performance, in terms of ductility, stiffness and strength, e.g. the "plastic" members of MCS – (S235 to S355) will dissipate the seismic energy, acting like "structural fuses", while the "elastic" members (HSS - S460 to S690), provided with adequate overstrength, will have the capacity to carry the supplementary stresses, following the redistribution of forces after appearance of plastic hinges. Such a structure is termed dual-steel structure. When braced frames of removable MCS dissipative members are used, such as the links in EBF, Buckling Restrained Braces in CBF or Shear Walls in MRF systems, the elastic HSS part of the structure has a beneficial restoring effect after earthquake enabling to replace the "fuses". Dual-steel approach can be considered for beam-to column connections, too, on the same philosophy related to the role of ductile and brittle components. The paper summarizes the numerical and experimental results obtained on this subject in the Department of Steel Structures and Structural Mechanics at the Politehnica University of Timisoara.*

1 INTRODUCTION

Multi-storey steel buildings are assigned to one of the following structural types, depending to the behavior of their lateral force resisting systems [1]:

- moment resisting frames (MRF), in which the horizontal forces are mainly resisted by members acting essentially in flexural mode; for such structures the performance of MR joints is crucial;
- frames with concentric bracings (CBF), in which the horizontal forces are mainly resisted by members subjected to axial forces;
- frames with eccentric bracings (EBF), in which the horizontal forces are mainly resisted by axially loaded members, but where the eccentricity of the layout is such that energy can be dissipated in seismic links by means of either cyclic bending or cyclic shear;
- moment resisting frames combined with dissipative shear walls (SW), which resist lateral forces by shear.

Usually, current building frames are Dual-Structures (DS) obtained by combination of a MRF with one of the lateral resisting systems, eg. MRF + CBF, MRF + EBF, MRF + SW.

Each of these structural systems dissipates a part of the seismic energy imparted in the structure through plastic deformations in the dissipative zones of the ductile members (i.e. beams in MRF, links in EBF or braces in CBF). The other members should remain in the linear range of response because nonlinear response is not feasible (i.e. columns). In order to avoid the development of plastic hinges in

these non-dissipative members, they must be provided with sufficient overstrength. To ensure this overstrength, European seismic design code EN1998, amplifies the design forces and moments by a multiplier equal to $1,1\gamma_{ov}$, where 1.1 takes into account for stress hardening, γ_{ov} is the overstrength factor and Ω is the ratio between the plastic resistance and the design value of the force in the dissipative member. In case of HSS structures, the values of factors composing this multiplier need to be very carefully analyzed. For some structural configurations (i.e. CBFs), the Ω factor may result considerably high, due to the fact that other non-seismic combinations (e.g. wind load) could be critical. A similar approach is also used in the AISC 2005 [2], where this factor may reach a value of 3 for some structural types. Even though, the verification of the non-dissipative members using such amplified forces do not guarantee they will behave entirely in the elastic range.

In order to get an economic design of the structure is necessary to keep the stresses quite low in the “dissipative” members using lower yield steel, and therefore to reduce the demand in the “non-dissipative” members, made by higher yield strength steel but still current. Such a solution has been recently applied to the design of a 26 story steel building frame in Bucharest, where lower yield strength steel S235 was used for the dissipative braces in the CBFs, while the other members were of S355 [3]. If this option is not possible, the alternative is to increase the strength of the non-dissipative members by using heavier sections or by using higher yield strength steel. For MRF structures, first option is recommended, as this will lead to an increase of the stiffness, which in many cases is critical in the seismic design, but for braced structures or for dual structures, this will lead to a stress concentration in the non-dissipative members (i.e. columns). For these structures, the adoption of high strength steel in the non-dissipative members (e.g. to remain in elastic range during the earthquake) seems to be more likely. However, previous results obtained by Dubina et al [4] have shown that for MRF structures, strengthening of columns by using HSS may be effective to avoid column failure in case of “near-collapse” state. This may also improve robustness of structure in case of other extreme loads (e.g. impact, blast). In case of such Dual Steel Frames, particular care is needed for the proper location and seizing of member sections of different materials, as well as for their connections. The design target is to obtain a dissipative structure, composed by “plastic” and “elastic” members, able to form a full global plastic mechanism at the failure, in which the history of occurrence of plastic hinges in ductile members can be reliable controlled by design procedures. To sustain these assumptions, a numerical study developed on DS of *conventional* CBF and EBF and on *non-conventional* braced systems, e.g. EBF of bolted removable links, CBF of Buckling Restrained Braces (BRB) and MRF of Steel Plate Shear Walls (SPSW), is presented. These so called “non-conventional” systems use dissipative components made by Mild Carbon Steel (MCS), which act as “seismic fuses” and are sacrificial member, which after a strong earthquake can be replaced.

2 SEISMIC PERFORMANCE OF DUAL STEEL FRAMES

2.1 Dual steel frames’ modeling and design

Four building frame typologies of eight and sixteen story, respectively, are considered [5]. The four lateral load resisting systems are: Eccentrically Braced Frames (EBF), Centrally V Braced Frames (CBF), Buckling Restrained Braced Frames (BRB) and Shear Walls (SW) (Figure 1). They are made by European H-shaped profiles. EBF, CBF and BRB systems have three bays of 6m. SW system has exterior moment frames bays of 5.0m, interior moment frame bay of 3.0m and shear wall bays of 2.5m. All structures have equal storey heights of 3.5m. Each building structure use different combinations of Mild Carbon Steel S235 and High Strength Steel S460. The design was carried out according to EN1993-1 [6], EN1998-1 and P100-1/2006 (Romanian seismic design code, aligned to EN1998-1) [7]. A 4 kN/m^2 dead load on the typical floor and 3.5 kN/m^2 for the roof were considered, while the live load amounts 2.0 kN/m^2 . The buildings are located in a moderate to high risk seismic area (i.e. the Romanian capital, Bucharest), which is characterized by a design peak ground acceleration for a returning period of 100 years equal to 0.24g and soft soil conditions, with $T_c=1.6 \text{ sec}$. It is noteworthy the long corner period of

the soil, which in this case may affect flexible structures. In such a case, there is a large demand in terms of plastic deformation capacity for dissipatively designed components, while it is very difficult to keep elastic the non-dissipative ones. For serviceability check, the returning period is 30 years (peak ground acceleration equal to 0.12g), while for collapse prevention it is 475 years (peak ground acceleration equal to 0.36g) (P100-1, 2006). Interstorey drift limitation of 0.008 of the storey height was considered for the serviceability verifications.

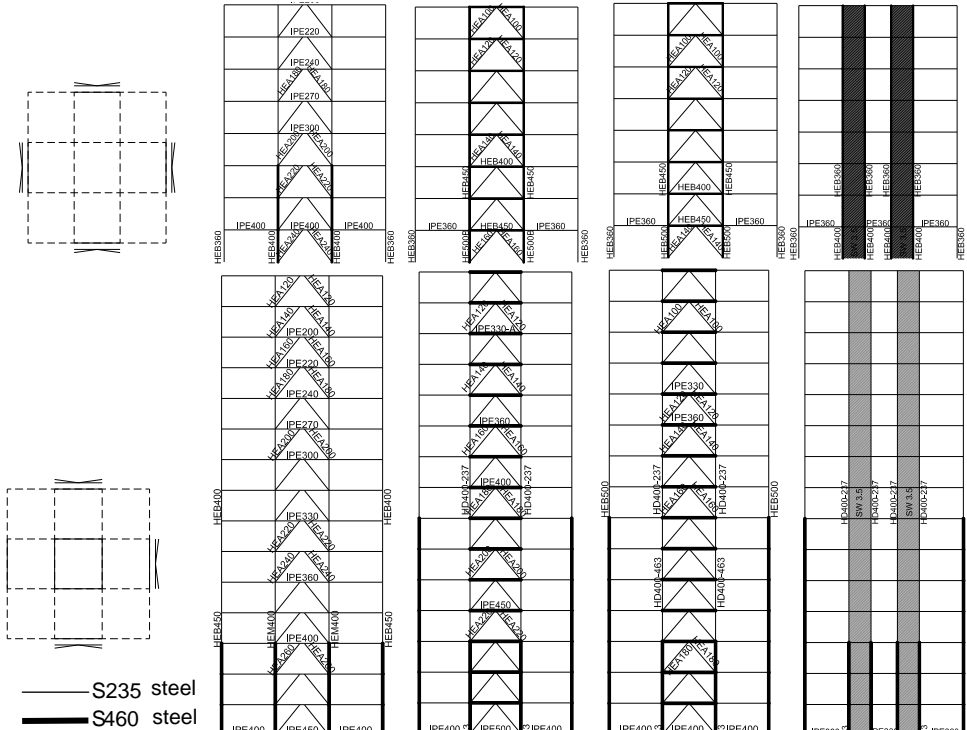


Figure 1. Frame systems: (a) plan view and elevation of EBF8, CBF8, BRB8 and SW8 structures; (b) plan view and elevation of EBF16, CBF16, BRB16 and SW16 structures

According to EN1998-1, the maximum value of the reduction factor q for dual frame systems of moment frames and eccentrically braced frames (MRF+EBF) is equal to 6. For dual frame systems made from moment frames and centrally braced frames (MRF+CBF), q factor amounts 4.8. For dual frame systems of moment frames and buckling restrained braces (MRF+BRB) and moment frames and shear walls (MRF+SW), EN1998-1 does not provide any recommendations regarding the q factor. For these structural systems, AISC 2005 provisions were taken as guidance. According to the later code, the reduction factor for MRF+BRB systems and MRF+SW is similar to that of special moment frames. Concluding, the design was based on a q factor equal to 6, excepting the MRF+CBF, which was designed for q equal to 4.8. For designing the non-dissipative members, EN1998-1 and P100-1/2006 amplifies the design seismic action by a multiplicative factor $1.1\gamma_{ov} \Omega$, where γ_{ov} is equal to 1.25. Unlike EN1998-1, which considers Ω as the minimum value of Ω_i among all dissipative members, Romanian code P100-1/2006 suggests the use of maximum value. A similar approach is also employed in AISC 2005, where the multiplicative factor $1.1\gamma_{ov} \Omega$ is replaced by a unique factor Ω_0 , called the overstrength factor. AISC

2005 and P100-1/2006 also contain values of multiplicative factors to be used in design, which ranges between 2.0 and 2.5. Table 1 presents the multiplicative factors for each structural system obtained by calculation. The overstrength factors Ω range between 1.90 and 2.90 for eight story structures and between 1.70 and 2.90 for sixteen story structures. For the eight-story building, two exterior bays of braces or shear walls on each exterior frames were necessary. For sixteen story building, the larger demand in lateral resisting capacity leads to braces or shear walls in all for bays.

The four structural systems were designed for similar base shear force capacities, with the exception of EBF, which were designed for lower capacities. The first mode periods for eight and sixteen story structures are presented in Table 1. It may be seen the four structural systems amount almost identical the first-mode periods.

Table 1. First mode periods and multiplicative factors for the structures

Structure	EBF8	CBF8	BRB8	SW8
1.1γov Ω	2.2	2.2	1.9	2.9
Period, [sec]	0.92	0.97	0.97	1.00
Structure	EBF16	CBF16	BRB16	SW16
1.1γov Ω	2.9	1.7	2.1	2.5
Period, [sec]	1.79	1.53	1.61	1.61

Beams and columns were modelled with plastic hinges located at both ends. In order to take into account the buckling of the diagonals in compression, the post buckling resistance of the brace in compression was set $0.2N_{b,Rd}$ (Figure 2.a), where $A_f y$ is the tensile yield resistance and $N_{b,Rd}$ is the buckling resistance for compression [8]. For the braces of the BRB systems, similar behaviour in tension and compression was adopted, as the buckling in compression is prevented (Figure 2.b). The inelastic shear link element model used for the EBF systems was based on the proposal of Ricles and Popov [9]. As the original model consisted in four linear branches, it was adapted to the trilinear envelope curve available in SAP2000 [10]. A rigid plastic behaviour was adopted till the attainment of the shear plastic capacity.

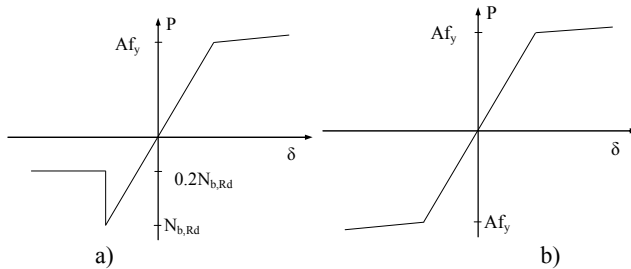


Figure 2. Response of bracing members: a) conventional brace; b) buckling restrained brace

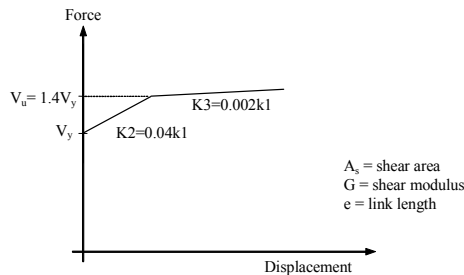


Figure 3. Force – displacement relationships for shear link element

For the shear wall structures (SW), non-compact shear walls, with the slenderness ratio h/t_w larger than λ_p but smaller than λ_r were selected (Figure 4) [11], where k_v is given by:

$$k_v = 5 + \frac{5}{(a/h)^2} = 5 \text{ when } a/h > 3.0 \text{ or } a/h > \left[260/(h/t_w)\right]^2 \quad (1)$$

where a is the distance between tension fields

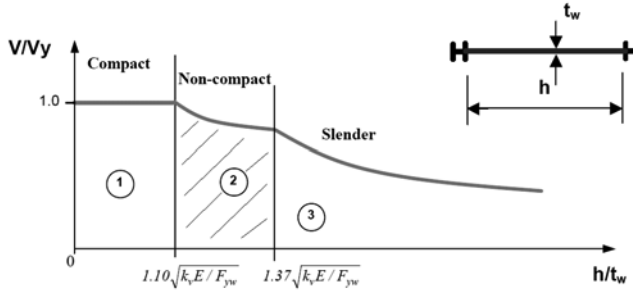


Figure 4. The regions of behaviour of the steel shear walls

The walls framed within this category are expected to buckle, while some shear yielding has already taken place. In this case, the story shear is resisted by the horizontal components of the tension and compression diagonal forces. In order to model the steel shear walls, Thorburn et al. [12], replaced the steel plates by a series of truss members (strips), parallel to tension fields (Figure 5). In this model, the infill steel plate is modelled as a series of tension-only strips oriented at the same angle of inclination, α , as the tension field. Studies have shown that ten strips per panel adequately represent the tension field action developed in the plate. Driver et al. [13] noted that there were certain phenomena present in steel plate shear wall behaviour that are not captured by the strip model. In their study, a compression strut oriented in the opposite diagonal direction to that of the tension strips was introduced. Moreover, a discrete axial hinge that includes the effects of deterioration was provided only for the two tension strips that intersect the frame closest to the opposite corners of the steel plate shear wall panel, as shown in Figure 5. The equation for the area of the compression strut is as follows:

$$A = \frac{tL \sin^2 2\alpha}{2 \sin \phi \sin 2\phi} \quad (2)$$

where

- ϕ is the acute angle of the brace with respect to the column;
- L is the centre-to-centre distance of columns;
- α is the angle of inclination of the average principle tensile stresses in the infill plate with respect to the boundary column;
- t is the infill plate thickness.

The equation for ϕ is as follows:

$$\tan \phi = \sqrt[4]{\frac{1 + tL/2A_c}{1 + th(1/A_b + h^3/360I_cL)}} \quad (3)$$

The width and spacing of the pin-ended tension and deterioration strips for each panel, based on ten strips per panel, were calculated to determine the area of each strip. The area calculated for the

compression strut is equally distributed among the tension strips. Figure 6 presents the typical behaviour for axial tension strip hinge, compression strut hinge and deterioration strip hinge.

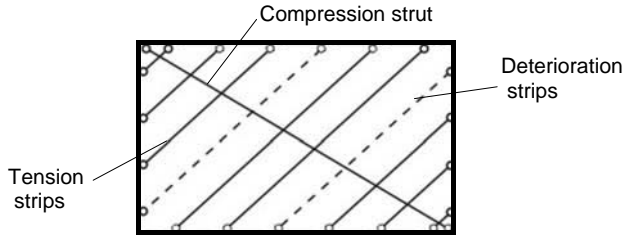


Figure 5. Strip model

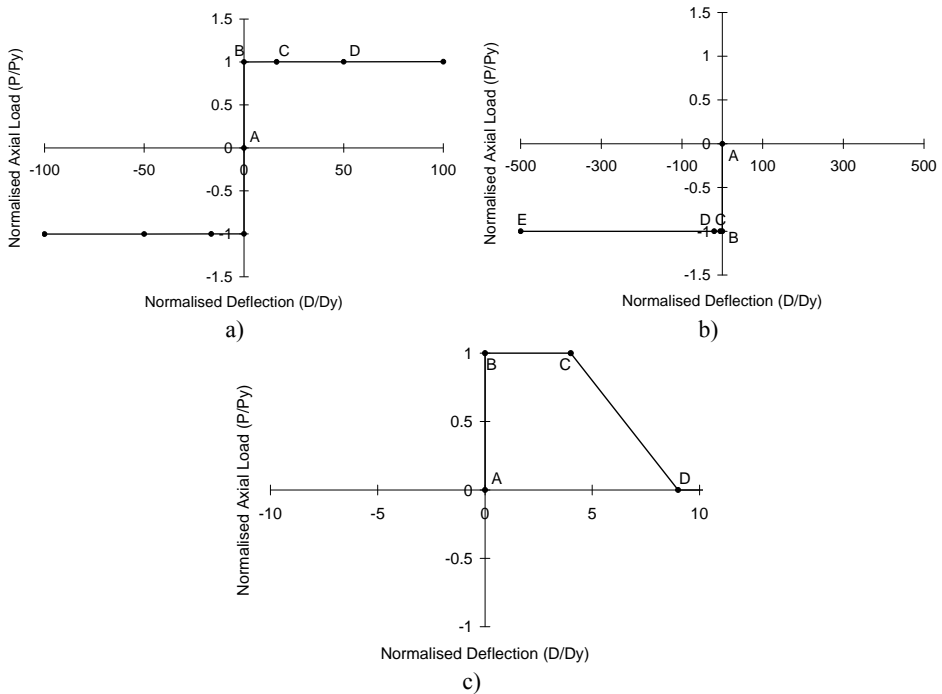


Figure 6. Axial hinge definitions: a) tension strip (infill plate); b) compression strut; c) deterioration hinge

2.2 Performance Based Evaluation

The nonlinear response of the structures was analysed using the N2 method [14]. This method combines the push-over analysis of a multi-degree of freedom model (MDOF) with the response spectrum analysis of a single degree of freedom system (SDOF). The elastic acceleration response spectrum was determined according to Romanian seismic code P100-1/2006, for a peak ground acceleration of 0.24g. The lateral force, used in the push-over analysis, has a “uniform” pattern and is proportional to mass, regardless of elevation (uniform response acceleration). The non-linear analysis was performed with SAP2000 computer program. Table 2 shows the values of target displacement, D_t , for the studied frames, calculated using N2 method.

Table 2. Target displacement, D_t , for the MDOF systems for ULS

Structure	EBF8	CBF8	BRB8	SW8
D_t , [m]	0.34	0.29	0.31	0.32
Structure	EBF16	CBF16	BRB16	SW16
D_t , [m]	0.64	0.49	0.53	0.62

Three performance levels were considered: serviceability limit state (SLS), ultimate limit state (ULS) and collapse prevention (CPLS) limit state. Intensity of earthquake action at the ULS is equal to the design one (intensity factor $\lambda = 1.0$). Ground motion intensity at the SLS is reduced to $\lambda = 0.5$ (similar to $v = 0.5$ in EN 1998-1), while for the CPLS limit state was increased to $\lambda = 1.5$ [8]. Based on [8], the following acceptance criteria were considered in the study:

- link deformations at SLS, ULS and CPLS are $\gamma_u=0.005\text{rad}$, $\gamma_u=0.11\text{rad}$ and $\gamma_u=0.14\text{rad}$.
- for conventional braces in compression (except EBF braces), plastic deformations at SLS, ULS and CPLS are $0.25\Delta_c$, $5\Delta_c$ and $7\Delta_c$, where Δ_c is the axial deformation at expected buckling load.
- for conventional braces in tension (except EBF braces), plastic deformations at SLS, ULS and CPLS are $0.25\Delta_t$, $7\Delta_t$ and $9\Delta_t$, where Δ_t is the axial deformation at expected tensile yielding load.
- for beams in flexure, the plastic rotation at ULS and CPLS are $6\theta_y$ and $8\theta_y$, where θ_y is the yield rotation
- for columns in flexure, the plastic rotation at ULS and CPLS are $5\theta_y$ and $6.5\theta_y$, where θ_y is the yield rotation

The performance is assessed by comparing the capacity of the structure, obtained from the push-over analysis, with the seismic demand expressed by the target displacement. Pushover curves for the EBF, CBF, BRB and SW structures and the occurrence of plastic hinges up to the target point are shown in Figure 6 and Figure 7. Table 3 presents the interstory drift demands for SLS and Table 4 presents the plastic deformations demand in members for the SLS, ULS and CPLS.

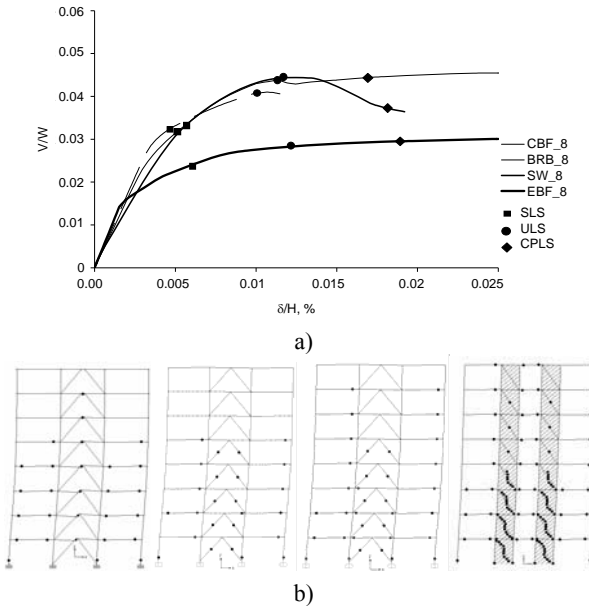


Figure 6. Pushover curves (normalized base shear vs. normalized top displacement) for eight story buildings a) and plastic hinges at ULS for EBF8, CBF8, BRB8 and SW8 structures b)

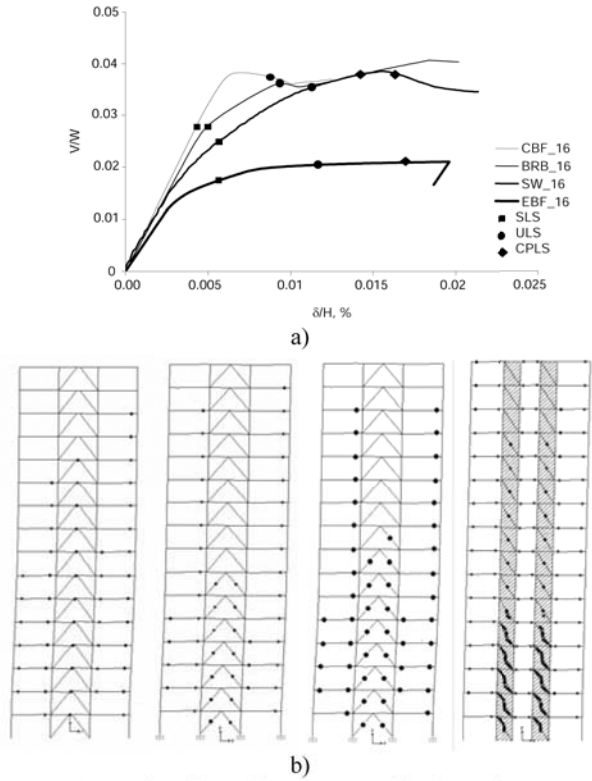


Figure 7. Pushover curves (normalized base shear vs. normalized top displacement) for sixteen story buildings a) and plastic hinges at ULS for EBF16, CBF16, BRB16 and SW16 structures b)

Table 3. Interstorey drift demands for SLS

Structure	EBF8	CBF8	BRB8	SW8
δ/H_s , %	0.008	0.007	0.008	0.007
Structure	EBF16	CBF16	BRB16	SW16
δ/H_s , %	0.008	0.005	0.006	0.007

First of all, before detailing the comparative analysis of studied frames, it is important to observe that no plastic hinges occur in columns for 15 story frames, even for CPLS, excepting conventional CBF system. For 8 story frames, practically no plastic hinges appear in columns up to ULS (the values of plastic hinge deformation demands in Table 4 are very low), which is for sure that, with plastic deformation recorded for CPLS stage, the frames are safely standing up, but again, excepting CBF system.

In comparison with the centrally braced structures (using conventional braces CBF and buckling restrained braces BRB), the ones using eccentrically braces (EBF) and shear walls (SW) are characterised by lower stiffness. Base shear force capacity is very similar for CBF, BRB and SW structures, implying similar design strength under seismic action. Lower base shear force capacities are recorded for EBF structures. Displacements demands for SLS are lower than the interstorey drift limitation of $0.008H_s$ used in design (Table 3). Structures designed using the dissipative approach, may experience structural damage even under moderate (SLS) earthquake. This is clearly seen in Table 4, where plastic

deformation demands in members are presented. Plastic deformations in dissipative members indicate a moderate damage to the structure at SLS.

All structures satisfy the criteria for ULS. Plastic deformation demands in beams are more severe for EBF and SW compared to CBF and BRB, and plastic mechanisms develop almost on entire height of the structures. Shear wall frames show a very good ductility, comparable to eccentrically braced ones, but also providing a higher stiffness. For sixteen story buildings, no plastic hinges are recorded in the columns, while for eight story buildings plastic hinges are recorded at the bottom part of the first story columns. This shows that in case of higher buildings, when the contribution of the gravity loads (i.e. dead loads, live loads) is lower, the Ω factor is more effective in design of non-dissipative members. Dissipation capacity shown by the structures confirms the reduction factors q used in design. Ductility of EBF, BRB and SW structures is similar to that of MRF, while CBF proved to be less ductile.

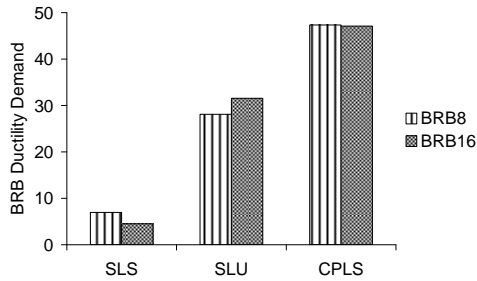


Figure 8. Ductility Demand Ratios for the buckling restrained braces

Table 4: Plastic deformation demands in members at SLS ($\lambda=0.5$), ULS ($\lambda=1.0$) and CPLS ($\lambda=1.5$)

	beams				columns				links	braces	
	[rad]				[rad]				[rad]		
	EBF8	CBF8	BRB8	SW8	EBF8	CBF8	BRB8	SW8	EBF8	CBF8	BRB8
SLS	0.004	0.0013	0.0012	0.005	-	-	-	-	0.04	0.001	0.003
ULS	0.018	0.016	0.016	0.016	0.006	0.002	0.002	0.004	0.1	0.043	0.0034
CPLS	0.027	PF*	0.035	0.038	0.01	PF*	0.03	0.033	0.15	PF*	0.094
	EBF15	CBF15	BRB15	SW15	EBF15	CBF15	BRB15	SW15	EBF15	CBF15	BRB15
SLS	0.007	0.0004	0.007	0.007	-	-	-	-	0.037	-	0.0038
ULS	0.021	0.013	0.015	0.017	-	-	-	-	0.11	0.044	0.028
CPLS	0.033	PF*	0.028	0.027	-	PF*	-	-	0.165	PF*	0.067

* PF – premature failure following the buckling of braces

Structures perform well till the attainment of the target displacement at CPLS, excepting CBF systems, which fail prematurely, mainly due to the failure of the braces in compression. When conventional braces are replaced by BRBs, the performance is improved and the performance level of collapse prevention is reached.

In case of EBF structures, plastic rotation demands in links exceed the rotation capacity. However, experimental tests on such elements have shown that in case of very short links, plastic rotation capacity may reach 0.17-0.20 rad [15]. The ductility demands in the buckling restrained braces are plotted in Figure 8. Experimental investigation on such type of members has shown the ductility of braces may exceed 25-30, depending on the material properties [16].

3. DUAL STEEL ECCENTRICALLY BRACED FRAMES OF REMOVABLE LINKS: PERFORMANCE AND RECENTERING CAPACITY

3.1 Removable link concept

As stated in Introduction, there are many possible solutions for structures with removable dissipative members. Application of this principle to eccentrically braced frames (EBFs), where links act as dissipative fuses, is presented in Figure 9 [17], [15]. The connection of the link to the beam is realized by a flush end-plate and high-strength friction grip bolts. In order to isolate inelastic deformations in removable dissipative elements only, these elements may be realised using lower yield steel. A similar effect can be obtained by using high strength steel in non-dissipative elements. The main advantage over special dissipative devices is the fact that removable links can be designed using methods readily available to structural engineers and can be fabricated and erected using standard procedures.

Bolted links for eccentrically braced frames were previously investigated by [18], [19] and [20].

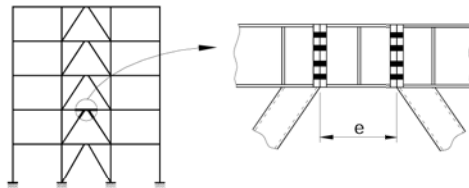


Figure 9. The bolted link concept

Two series of experimental tests on removable link assemblies were carried out at the "Politehnica" University of Timisoara in order to determine cyclic performance of bolted links and to check the feasibility of the removable link solution [17], [15]. The first series of tests was realised on isolated links (see Figure 10a-b), while the second one on full-scale model of a single bay and single storey eccentrically braced frame with removable link (see Figure 10c). Tests on links showed an important influence of the connection on the total response of the bolted link, in terms of stiffness, strength and overall hysteretic response. Shorter links were found to be suitable for the bolted solution, as plastic deformations were constrained to the link, while the connection response was almost elastic, allowing for an easy replacement of the damaged link. At the frame level, the experimental tests showed that the removable link solution is feasible. Inelastic deformations were constrained to the removable links alone, all other frame members and connections remaining in the elastic range. Additionally, it was possible to replace the damaged removable links with new elements.

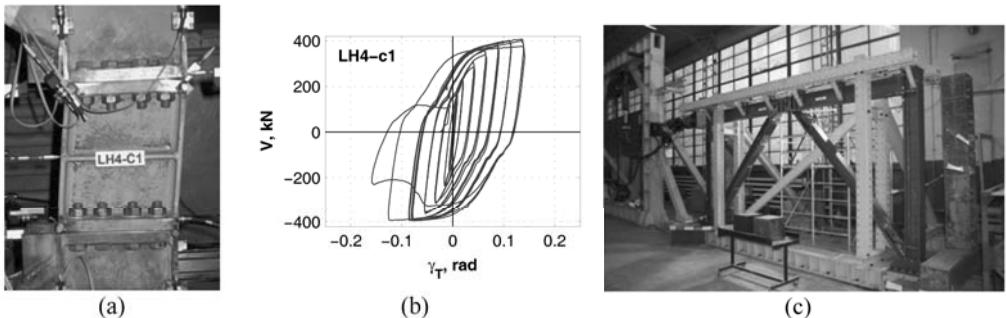


Figure 10. Experimental test on removable bolted link – LH4-c1 specimen (a); force-deformation relationship $V-\gamma_T$ of the same specimen (b) and tests on full-scale frame with bolted links (c)

For a system containing removable dissipative elements to be efficient, it must fulfil to requirements. The first one consists in isolating inelastic to removable elements only, assuring an easy repair of the damaged structure. Capacity design rules incorporated in modern design codes can be used in order to attain this objective. The second requirement is related to the possibility to replace damaged dissipative elements that can be difficult to realise if the structure has experienced large permanent deformations.

Several researchers investigated seismic performance of dual systems, consisting of rigid and flexible subsystems. According to these studies, the potential benefits of dual structural configurations may be summarised as follows:

- Efficient earthquake resistance due to prevention of excessive development of drifts in the flexible subsystem, and dissipation of seismic energy in the rigid subsystem by plastic deformations.
- Alternative load path to seismic loading provided by the secondary subsystem (the flexible one) in the case of failure of the primary subsystem (the rigid one)

In order to analyse the factors controlling the two requirements for structures with removable dissipative members (e.g. isolation of damage and limitation of permanent drifts), it is useful to consider a simple dual system consisting of two inelastic springs connected in parallel (see Figure 11a).

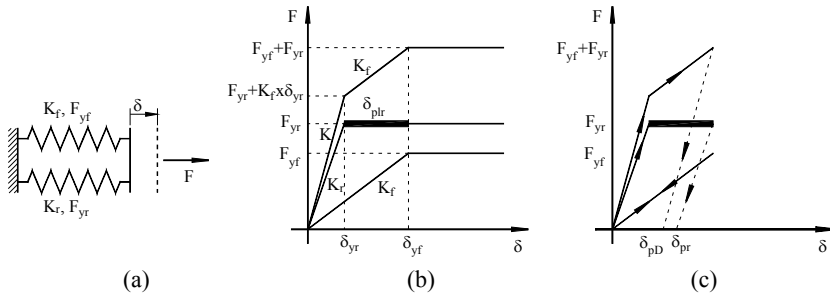


Figure 11. Simplified model of a generalized dual system

Provided that the flexible subsystem is not very weak, plastic deformations appear first in the rigid subsystem. Therefore, an efficient dual system must be realised by combining a rigid and ductile subsystem, with a flexible subsystem. In order to maximize system performance, plastic deformations in the flexible subsystem should be avoided. At the limit, when the yield force F_{yf} and yield displacement δ_{yf} are attained in the flexible subsystem, the rigid subsystem experiences the yield force F_{yr} and the total displacement $\delta_{yr} + \delta_{plr}$ (see Figure 11b). Equating the two displacements:

$$\delta_{yf} = \delta_{yr} + \delta_{plr}$$

and considering the relationship between force and deformation:

$$F = k \cdot \delta$$

it can be shown that

$$\mu_D = \frac{\delta_{yr} + \delta_{plr}}{\delta_{yr}} = \frac{\delta_{yf}}{\delta_{yr}} = \frac{F_{yf}}{F_{yr}} \cdot \frac{K_{yr}}{K_{yf}}$$

The notation μ_D represents the "useful" ductility of the rigid subsystem, for which the flexible subsystem still responds in the elastic range. It can be observed that there are two factors that need to be considered in order to obtain a ductile dual system with plastic deformations isolated in the rigid subsystem alone. The first one is the ratio between the yield strength of the flexible and rigid subsystems (F_{yf}/F_{yr}), while the second one is the ratio between the stiffness of the rigid subsystem and the one of the flexible subsystem. The larger are these two factors, the larger is the "useful" ductility μ_D of the dual system.

The second objective, of limitation of permanent deformations, is not easily attainable. Though the dual configuration is results in smaller permanent drifts δ_{pD} in comparison with permanent deformations of the rigid system alone δ_{pr} (see Figure 11c), they are not eliminated completely after unloading. However, permanent deformations can be eliminated if the rigid subsystem is realised to be removable. Once it is replaced after the system experienced inelastic deformations, the flexible subsystem alone provides the necessary stiffness and strength to the system. If the flexible subsystem is still in the elastic range, it will return the system to the initial position, implying zero permanent deformations.

Considering the above, practical implementation of the concept of removable dissipative elements and dual systems can be obtained by combining eccentrically braced frames with removable links (the rigid subsystem) and moment-resisting frames (flexible subsystem).

3.2 Evaluation of performance of EBFs with removable links

In order to assess seismic performance of eccentrically braced frames with removable links, a medium rise structure was investigated as a case study. The building has 3x3 bays of 6 m each, and 8 storeys (see Figure 12).

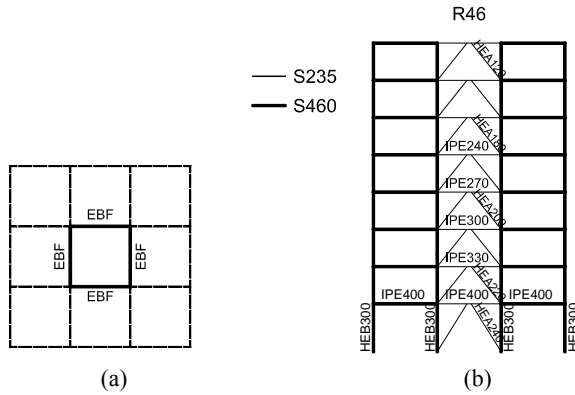


Figure 12. Structural layout: (a) plan view; (b) elevation dual frame R46

All storeys are 3.5 m, except the first one, which equals 4.5 m. The design was carried out according to EN 1993, EN 1998 (2004) and P100-1/2006. A 4 kN/m² dead load on the typical floor and 3.5 kN/m² for the roof were considered, while the live load amounted 2.0 kN/m². The building location is again Bucharest (PGA = 0.24g, T_C=1.6 sec). A behaviour factor q=6, and an interstorey drift limitation of 0.008 of the storey height were considered in design. Columns are of fixed base and rigid beam to column connections were assumed.

The Moment Resisting (MR) part of the frame DS (e.g. the “elastic” one) is realised of S460 steel, while the EBF part (e.g. the “plastic” one), including the removable link is of S235.

Experimental results showed that for very short links the flush end plate connection remained essentially elastic. For these links the strength was governed by the shear strength of the link, and the cyclic response was not affected by strength and stiffness degradation in the connection like for longer links. For the numerical investigation, very short links were used, with e=400mm, characterised by negligible influence of connection on cyclic response of the removable link. Therefore, only the stiffness of the removable link was considered to be affected by the flexibility of the bolted link-beam connection. Based on experimental tests, an equivalent stiffness of 0.25 of the theoretical shear stiffness of continuous links was considered for bolted links. In order to reduce inelastic deformations in members outside links, higher steel grade was used in these members.

Inelastic analysis of the frames was realised using DRAIN-3DX computer program. Beams, columns and braces were modelled with fibre hinge beam-column elements, with plastic zones located at the ends.

Nominal steel characteristics were used. Elastic-perfectly plastic behaviour was assumed, without strength and stiffness degradation. Buckling of braces was not considered explicitly in the model due to the limitations of the inelastic beam-column element available in the program. However, compression force demand in braces was checked against buckling strength of braces, computed according to EN 1993-1-1 provisions using nominal material characteristics and a buckling length equal to 0.8 times the clear length of the brace, corresponding to braces welded directly to the column and beam.

The inelastic shear link element model was based on the one proposed by Ricles and Popov [9]. As the original model consisted in four linear branches, it was adapted to the trilinear envelope curve available in Drain-3dx. It consists of an initial elastic response up to yield force, followed by a strain hardening range with a stiffness of 4% from the initial one up to a force 1.4 times the yield one, with a strain hardening behaviour afterwards at the 0.2% of the initial stiffness.

A set of seven ground motions were used. Spectral characteristics of the ground motions were modified by scaling Fourier amplitudes to match the target elastic spectrum from P100-1/2006, see Figure 13. This results in a group of semiartificial records representative to the seismic source affecting the building site and soft soil conditions in Bucharest. The procedure was based on the SIMQKE-1 program [21].

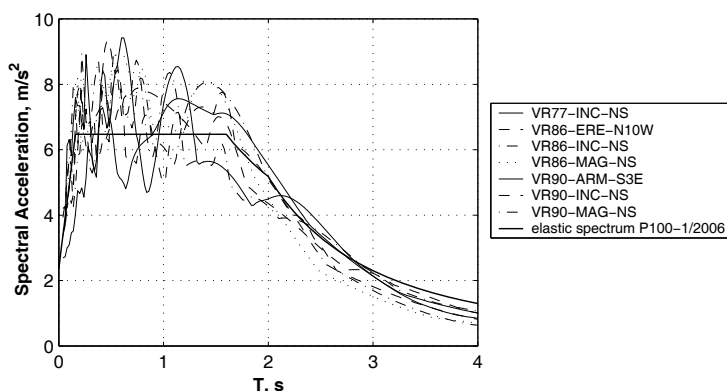


Figure 13. Elastic response spectra of semiartificial records and P100-1/2006 elastic spectrum.

In order to assess structural performance, an incremental dynamic analysis (IDA) was performed. Three performance levels were considered: serviceability limit state (SLS), ultimate limit state (ULS), and collapse prevention (CPLS) limit state. Intensity of earthquake action at the ULS was equal to the design one (intensity factor $\lambda = 1.0$). Ground motion intensity at the SLS was reduced to $\lambda = 0.5$ (according to $v = 0.5$ in EN 1998-1), while for the CPLS limit state was increased to $\lambda = 1.5$ (according to FEMA 356). Based on experimental results and FEMA 356 provisions, ultimate link deformations at ULS and CPLS were $\gamma_u = 0.11$ rad and $\gamma_u = 0.14$ rad, respectively.

Results of IDA are synthetically presented in Figure 14, in terms of maximum transient interstorey drift ratio (IDR) and maximum permanent IDR. The benefit of HSS for the structure with removable links (R46) is clearly identified in Figure 14b, giving the lowest values of permanent drifts up to intensity factors of $\lambda = 1.0 - 1.2$. Low permanent drifts allow easier replacement of damaged removable links. Maximum plastic deformation demands in members at SLS, ULS and CPLS are presented in Table 5. Structures designed using the dissipative approach, may experience structural damage even under moderate (SLS) earthquake. This can be seen in Figure 15, where plastic deformation demands in members are represented. One observes the plastic deformations outside the link are completely avoided for SLS stage, negligible for ULS and reduced for CPLS, so *quod erat demonstrandum*.

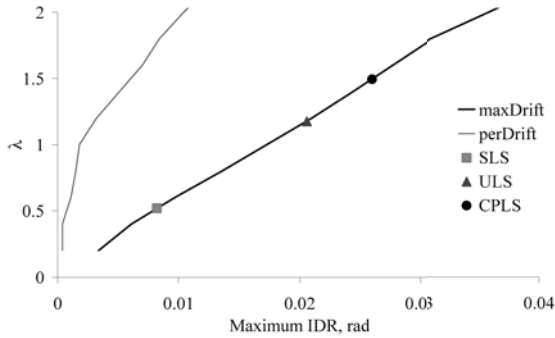


Figure 14. IDA curves: maximum and permanent drift vs. acceleration multiplier, average of all records

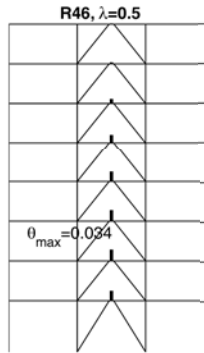


Figure 15. Plastic deformation demands in members at SLS ($\lambda = 0.5$) for the R46 structure, average of all records

Table 5. Plastic deformation demands in members at SLS ($\lambda = 0.5$), ULS ($\lambda = 1.0$) and CPLS ($\lambda = 1.5$) for the R46 structures, average of all records, [in rad]

	links	beams	columns
SLS	0.036	-	-
ULS	0.092	0.004	0.002
CPLS	0.145	0.014	0.008

3.3 Recentering capacity: study case

The main advantage of using removable dissipative members in dual-steel structures is to take benefit from possibility to replace those members after they consumed their fuse role. On this purpose, it is important to size correctly the structural components on the aim to keep small the residual drift and ensure the recentering of the structure after the earthquake. A case study will be used in order to provide evidence of the advantages of using removable links associated with HSS components in the elastic part of the dual framing.

In order to check the level of permanent forces and deformations, the test structure was designed according to EN 1993-1-1 and EN 1998-1 for typical gravity loadings and a peak ground acceleration of 0.24g, corresponding to soil conditions in Bucharest (Figure 16). A nonlinear time-history analysis was then performed on the test structure under the NS component of the Vrancea '77 ground motion record,

scaled in order to correspond to attainment of ultimate shear deformation in links (0.1 rad). Results from Table 6 present the normalized interstorey drift, link shear displacements and vertical relative displacements of the link ends along the building stories. In Table 7 the bending moment and shear force in the links are presented. In order to mark the residual (or permanent) deformations and stresses in the links, both maximum values and permanent values at the end of the analysis are presented.

Values of permanent deformations and lateral displacements in the structure are very small, compared to maximum values recorded during analysis. Thus, the maximum permanent interstorey drift amounts only to 5.5% of the maximum one, while permanent shear deformation amounts to 6.6% of the maximum plastic rotation. The residual vertical displacement between link ends is 2.7 mm only, which shows a very small residual plastic deformation in the link. Residual stresses are also low, bending moment amounts 9.7% of the maximum one, while shear force is just 1.8% of the maximum one. Based on these reduced values of residual stresses, it can be anticipated that the replacement of the damaged links is feasible, even without relaxing completely the links in shear by the flame cutting of the link web. As the beams outside the links remain elastic, the initial position can be completely regained after the damaged links are dismantled. Though this analysis was performed for a single seismic record, but which is very demanding, the results show that in many cases the flame cutting could be avoided. This research is part of an ongoing SERIES Project, "DUAREM". Within this project, the full scale structure will be tested pseudo-dynamically at JRC Ispra.

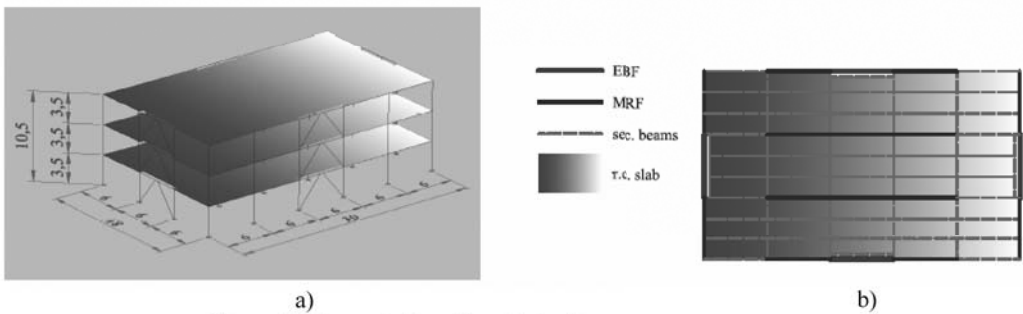


Figure 16. General view (a) and plan layout (b) of the structure.

Table 6. Values of interstorey drift and link rotation along the stories

	Relative interstorey drift [%Hs]		Links ends vertical displacement [mm]		Plastic rotation in links [rad]	
	maximum	permanent	maximum	permanent	maximum	permanent
1 st storey	0.82	0.045	40	2.7	0.10	0.0068
2 nd storey	0.61	0.029	26.1	1.6	0.06	0.004
3 rd storey	0.17	0.0008	7.8	0	0.019	0

Table 7. Values of bending moment and shear forces in links, along the stories

	Bending moment in links, ML, [kNm]		Shear force in links, VL [kN]	
	maximum	permanent	maximum	permanent
1 st storey	114.4	11.1	507.4	9.2
2 nd storey	97.0	4.4	444.5	1.03
3 rd storey	65.7	1.83	325.0	1.41

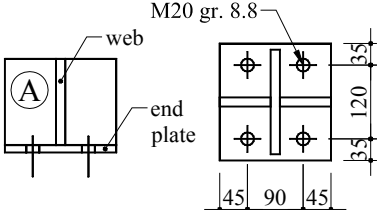
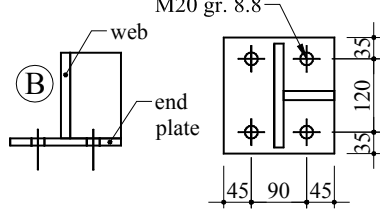
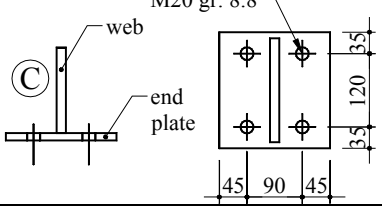
4. DUAL STEEL CONNECTIONS

When HSS is used in members designed to remain predominantly elastic, e.g. columns, or in end-plates of bolted beam to column joints, T-stub macro-components made of two steel grades are obtained. The performances of Dual-Steel bolted T-stub specimens were studied at the Politehnica University of Timisoara within a large experimental program.

The objective of the experimental program was to study the performance of welded and bolted end-plate beam-to-column joints realized with two different steel grades components. The experimental program consisted in tests on materials, weld details, T-stub components and beam to column joints. This section of the paper summarizes the investigations on T-stub components, only. Previous papers already presented the results and whole testing program [22], [23].

T-stubs are basic components of the component method used in EN 1993-1-8 [24] for evaluation of strength and stiffness of bolted end-plate beam to column joints. Both monotonic and alternating cyclic tests were performed on T-stub components obtained by welding S235 web plates to S235, S460 and S690 end-plates, using K beveled full-penetration welds (Table 8).

Table 8. T-stub characteristics

T-stub type	Label	Web	End-plate	Design failure mode
	TST-12A-S235	S235	S235 t = 12 mm	2
	TST-20A-S235	t=15 mm	S235 t = 20 mm	2 → 3
	TST-10A-S460		S460 t = 10 mm	2
	TST-16A-S460		S460 t = 16 mm	2 → 3
	TST-8A-S690		S690 t = 8 mm	2
	TST-12A-S690		S690 t = 12 mm	2 → 3
	TST-12B-S235	S235	S235 t = 12 mm	1 / 2
	TST-20B-S235	t=15 mm	S235 t = 20 mm	2 / 2 → 3
	TST-10B-S460		S460 t = 10 mm	1 / 2
	TST-16B-S460		S460 t = 16 mm	2 / 2 → 3
	TST-8B-S690		S690 t = 8 mm	1 / 2
	TST-12B-S690		S690 t = 12 mm	2 / 2 → 3
	TST-12C-S235	S235	S235 t = 12 mm	1
	TST-20C-S235	t=15 mm	S235 t = 20 mm	2
	TST-10C-S460		S460 t = 10 mm	1
	TST-16C-S460		S460 t = 16 mm	2
	TST-8C-S690		S690 t = 8 mm	1
	TST-12C-S690		S690 t = 12 mm	2

Notes:

- 1: One monotonic and two cyclic tests have been performed for each specimen type.
2. Failure modes according to EN 1993-1-8: 1) ductile, 2) semi-ductile, 3) brittle

On the purpose to obtain full strength rigid beam-to-column connections, outer stiffeners needs to be applied at the extended end-plate (Figure 17); consequently, double stiffened T-stub specimens are obtained (Type A in Table 8).

MAG welding was used, with G3Si1 (EN 440) electrodes for S235 to S235 welds, and ER 100S-

G/AWS A5.28 (LNM Moniva) for S235 to S460 and S690 welds. T-stubs were connected using M20 gr. 8.8 bolts. EN 1993-1.8 was used to obtain the design strength of T-stubs and failure modes. Thickness of end-plates was determined so that the unstiffened T-stub (type C) would fail in mode 1 (end-plate) and mode 2 (combined failure through end-plate bending and bolt fracture). The same end-plate thickness was then used for the stiffened T-stubs (type B and A), see Table 8.

Table 9 shows the measured average values of yield stress f_y , tensile strength f_u and elongation at rupture, A. One observes the value of elongation for S460 is significantly large. Bolts were tested in tension as well, showing an average ultimate strength of 862.6 N/mm². Loading was applied in displacement control under tension and force control under compression. Compressive force was chosen so as to prevent buckling of the specimen.

Table 9. Material properties

Nominal steel grade	f_y , N/mm ²	f_u , N/mm ²	A, %	Actual steel grade
S235	266	414	38	S235
S460	458	545	25	S460
S690	831	859	13	S690

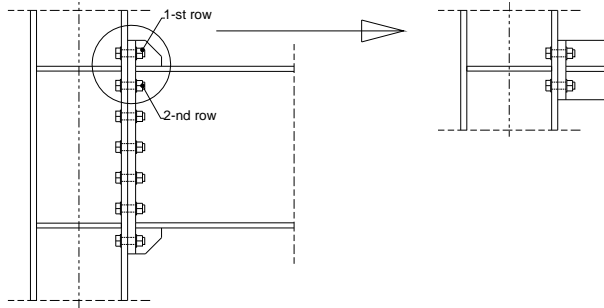


Figure 17. Assumption for A-type T-stub

For specimens of types B and C, it was not possible to have full reversible cycles due to the buckling. For stiffened T-stubs (eg. A or B), generally semi-ductile failure mode, 2, was obtained, except the case of thicker end-plate, even of S235 (MCS), when a brittle failure occurred. It seems the choice of thickness associated with steel grade is important in the conception of a proper connection, in order to obtain a good balance between strength, stiffness and ductility of components.

Figure 18 shows examples of the 3 types of observed failure modes, together with the corresponding force-displacement relationships of T-stub specimens. There were no significant differences in force values between failure modes of monotonic specimens and cyclic specimens, both agreeing with analytical predictions by EN 1993-1-8. It is clear the ductile mode is the weaker one, while the brittle mode 3 is the stronger. Figure 19a and Figure 19b show the comparison between monotonic and cyclic tests in terms of ultimate displacements D_u and experimental vs. predicted monotonic yield force F_y , respectively. Under monotonic loading, ultimate displacement was smaller for specimens of thicker end-plates that failed in modes 2 and 3 involving bolt failure. Cyclic loading reduced significantly ultimate displacement of specimens with thinner end-plates that failed in mode 1. This behavior is attributed to low-cycle fatigue that generated cracks in the HAZ near the welds, along yield lines. On the other hand, cyclic loading did not affect much ultimate displacement for specimens with thicker end-plates that failed in modes 2 and 3, governed by bolt response. It is interesting to note that specimens realized from high-strength end plates (S460 and S690, with lower elongation at rupture), had a ductility comparable with the one of specimens realized from mild carbon steel (S235).

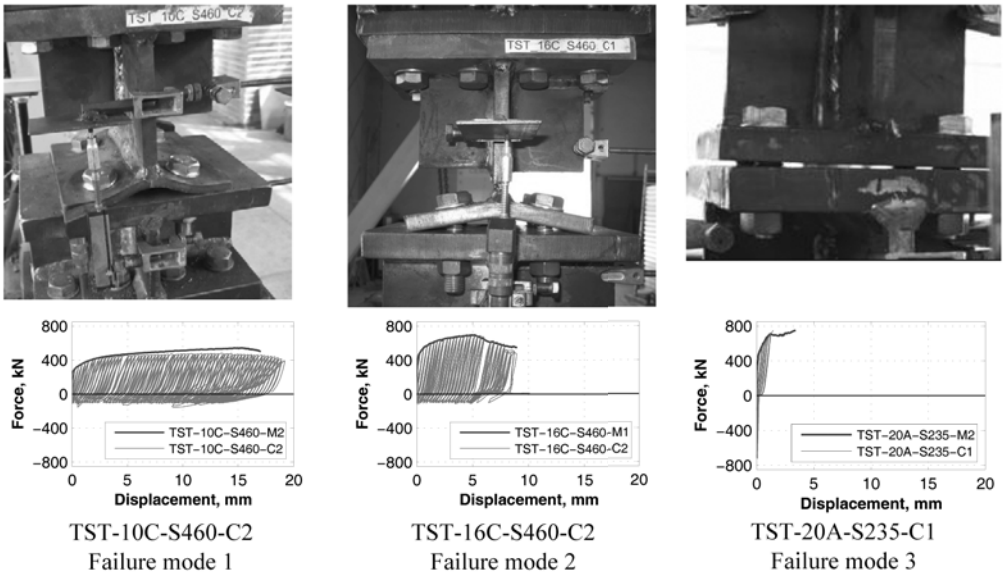


Figure 18. Examples of failure modes of T-stub specimens

In Table 10 and Figure 20 the interpretation of test results base on low-cycle approach is presented [25]. Based on these results, one concludes that, in general, no particular failure problems are met in case of Dual-Steel welded connections of the type used in extended end-plate bolted beam-to-column seismic resistant joints. If full strength Moment Resisting Joints are desired, they cannot be detailed and sized for failure Mode 1 of T-stubs, because it always leads to partial strength connections. Alternatively, the stronger Mode 3, the brittle one, is really dangerous, because the designed overstrength related to nominal yield strength of the MCS beam is often vanished by the real MCS yield strength of the material. So that still is need for connection ductility, even designed as full strength. Mode 2, when properly calibrated, enables to obtain both full strength and ductile beam to column joints. Playing with both steel grade and thickness of components, gives to obtaining beam to column joints with such properties.

One sees in Table 10 and Figure 20, this is, generally the case of TST-16A-S460, which is strong enough (Figure 19a) and has an acceptable energetic ductility (e.g. μ_E in Table 10). The paper presented in the Proceeding of SDSS 2010 Conference [26] proves that.

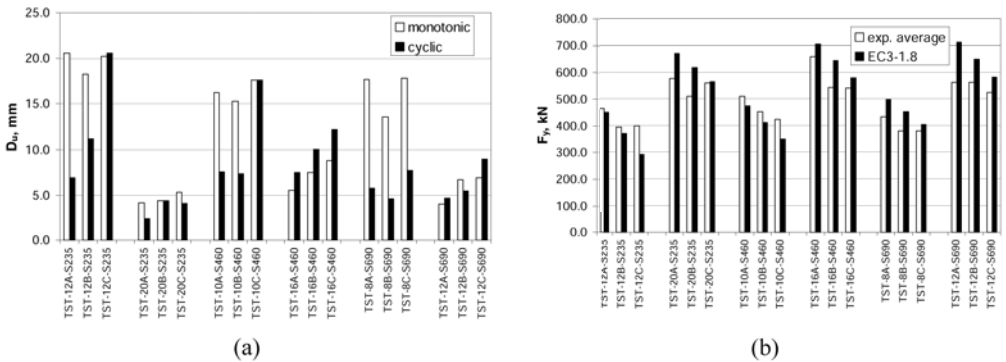


Figure 19. Interpretation of results

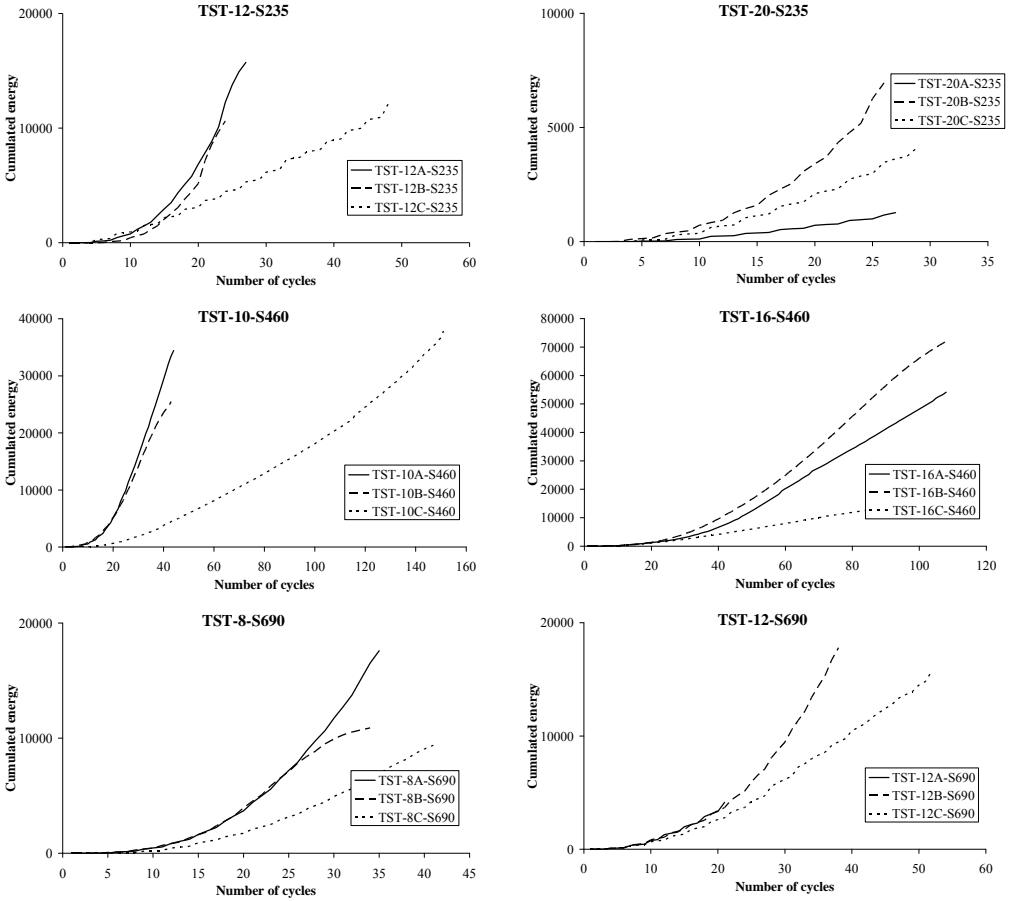


Figure 20. Cumulated energy

Table 10. Interpretation of cyclic tests in term of energy

Specimen	Nr. of cycles	$\Delta\sigma$ [N/mm ²]	$\Delta\sigma_C$ [N/mm ²]	$\mu_E=(E_u-E_v)/E_v$	Failure mode
TST-12A-S235	27	10367	247	670	1
TST-12B-S235	24	11146	255	523	1
TST-12C-S235	48	6060	175	583	1
TST-20A-S235	26	720	17	40	3
TST-20B-S235	26	4846	114	279	2→3
TST-20C-S235	28	2810	69	178	2
TST-10A-S460	45	12749	357	920	1
TST-10B-S460	43	10232	285	744	1
TST-10C-S460	151	10438	441	2435	1
TST-16A-S460	110	8296	315	1567	2

Table 10. (Continued)

Specimen	Nr. of cycles	$\Delta\sigma$ [N/mm ²]	$\Delta\sigma_c$ [N/mm ²]	$\mu_E=(E_u-E_v)/E_v$	Failure mode
TST-16B-S460	106	12614	478	2439	2
TST-16C-S460	89	3530	126	491	2
TST-8A-S690	35	16306	423	456	1
TST-8B-S690	34	11782	303	340	1
TST-8C-S690	41	18867	516	673	1
TST-12A-S690	21	5141	113	70	3
TST-12B-S690	38	15912	425	481	2
TST-12C-S690	52	10832	321	469	2

5. CONCLUDING REMARKS

Dual-Steel frames enable for a better control of seismic response of multistory buildings. Ductile MCS members can be designed as fuses and replaceable components, while the HSS members, designed to remain predominantly elastic during earthquakes and to provide alternative load distribution paths during earthquake, might provide a beneficial recentering capacity of the entire structure to keep lower the residual drift. A Performance Based Design approach can be successfully applied in order to obtain such a type of behavior. Also, following the same principle, Dual-Steel connections can be shaped and sized to supply both necessary ductility and overstrength to cover better the seismic demands for MR joints. There are no technological difficulties when HSS components are welded to the MCS ones.

6. REFERENCES

- [1] EN, 1998-1, 2004. Design provisions for earthquake resistance of structures - 1-1: General rules - Seismic actions and general requirements for structures, CEN, EN1998-1-1.
- [2] AISC 341-05, 2005. Seismic provisions for structural steel buildings. *American Institute for Steel Construction*, 2005
- [3] Dubina, D., Dinu, F., Stratan and Ciutina, A., "Analysis and design considerations regarding the project of Bucharest Tower International Steel Structure". *Proc. of ICMS 2006 Steel a new and traditional material for building*, Brasov, Romania, 2006, Taylor&Francis/Balkema, Leiden, The Netherlands, ISBN 10: 0 415 40817 2, Ed. D., Dubina, V. Ungureanu, 2006.
- [4] Dubină, D., Dinu, F., Zaharia, R., Ungureanu, V. and D. Grecea, D., "Opportunity and Effectiveness of using High Strength Steel in Seismic Resistant Building Frames". *Proc. of ICMS 2006 Internat. Conf. "Steel, a new and traditional material for building"*, Poiana Brasov, Romania, September 20-22, 2006, Taylor&Francis/Balkema, Leiden, The Netherlands, ISBN 10: 0 415 40817 2, Ed. D., Dubina, V. Ungureanu, 2006.
- [5] Dinu, F., Dubina, D. and Neagu, C., "A comparative analysis of performances of high strength steel dual frames of buckling restrained braces vs. dissipative shear walls". *Proc. of International Conference STESSA 2009: Behaviour of Steel Structures in Seismic Areas*, Philadelphia, 16-20 aug. 2009, CRC Press 2009, Ed. F.M. Mazzolani, J.M. Ricles, R. Sause, ISBN: 978-0-415-56326-0, 2009.
- [6] EN1993-1-1: Design of Steel Structures. Part 1-1: General rules and rules for buildings, CEN, Brussels, 2003.

- [7] P100-1/2006: Cod de proiectare seismică P100: Partea I, P100-1/2006: Prevederi de proiectare pentru clădiri, 2006 (in Romanian).
- [8] FEMA 356. Prestandard and commentary for the seismic rehabilitation of buildings. *Federal Emergency Management Agency and American Society of Civil Engineers*, Washington DC, USA, 2000.
- [9] Ricles J.M. & Popov, E.P. 1994. Inelastic link element for EBF seismic analysis, ASCE. *Journal of Structural Engineering*, 1994, Vol. 120, No. 2: 441-463.
- [10] SAP2000, Version 9, 2005. Computers and Structures Inc. University Avenue, Berkeley, California 94704, USA, 2005.
- [11] AISC 1999. Load and Resistance Factor Design Specification, American Institute of Steel Construction Inc., Chicago, 1999.
- [12] Thorburn, L. J., Kulak, G. L., and Montgomery, C. J., "Analysis of steel plate shear walls", *Structural Engineering Rep. No. 107*, Dept. of Civil Engineering, Univ. of Alberta, Edmonton, Alberta, Canada, 1983.
- [13] Driver, R. G., Kulak, G. L., Kennedy, D. J. L. and Elwi, A. E., "Seismic behavior of steel plate shear walls". *Structural Engineering Rep. No. 215*, Dept. of Civil Engineering, Univ. of Alberta, Edmonton, Alberta, Canada, 1999.
- [14] Fajfar, P., "A non linear analysis method for performance based seismic design", *Earthquake Spectra*, vol.16, no. 3, pp. 573-592, August 2000.
- [15] Stratan, A. and Dubina, D., "Bolted links for eccentrically braced steel frames", *Proc. of the Fifth Int. Workshop "Connections in Steel Structures V. Behaviour, Strength & Design"*, June 3-5, 2004. Ed. F.S.K. Bijlaard, A.M. Gresnigt, G.J. van der Vege. Delft University of Technology, Netherlands, 2004.
- [16] Bordea, S., Stratan, A. and Dubina, D., "Performance based evaluation of a RC frame strengthened with BRB steel braces", *PROHITECH '09 International Conference*, 21-24 June, 2009, Rome, Italy, 2009.
- [17] Dubina, D., Stratan, A. and Dinu, F., "Dual high-strength steel eccentrically braced frames with removable links". *Earthquake Engineering & Structural Dynamics*, Vol. 37, No. 15, p. 1703-1720, 2008.
- [18] Balut, N. and Gioncu, V., "Suggestion for an improved 'dog-bone' solution", *STESSA 2003, Proc. of the Conf. on Behaviour of Steel Structures in Seismic Areas*, 9-12 June 2003, Naples, Italy, Mazzolani (ed.), A.A. Balkema Publishers, p. 129-134, 2003.
- [19] Mansour, N., Christopoulos, C. and Tremblay, R., "Seismic design of EBF steel frames using replaceable nonlinear links", *STESSA 2006 – Mazzolani & Wada (eds)*, Taylor & Francis Group, London, p. 745-750, 2006.
- [20] Ghobarah, A. and Ramadan, T., "Bolted link-column joints in eccentrically braced frames", *Engineering Structures*, Vol.16 No.1: 33-41, 1994.
- [21] Gasparini, D.A., and Vanmarcke, E.H., "Simulated Earthquake Motions Compatible with Prescribed Response Spectra", Department of Civil Engineering, *Research Report R76-4*, Massachusetts Institute of Technology, Cambridge, Massachusetts, 1976.
- [22] Dubina, D., Stratan, A. Muntean, N. and Grecea, D. (2008a), "Dual-steel T-stub behavior under monotonic and cyclic loading", *ECCS/AISC Workshop: Connections in Steel Structures VI*, Chicago, Illinois, USA, June 23-55, 2008.
- [23] Dubina, D., Stratan, A. Muntean, N. and Dinu, F., "Experimental program for evaluation of Moment Beam-to-Column Joints of High Strength Steel Components", *ECCS/AISC Workshop: Connections in Steel Structures VI*, Chicago, Illinois, USA, June 23-55, 2008.
- [24] EN 1993-1.8. Design of steel structures. Part 1-8: Design of joints, European standard, 2003.

- [25] D. Dubina, D. Grecea, A. Stratan & N. Muntean, “Performance of dual-steel connections of high strength components under monotonic and cyclic loading”, *Proc. of International Conference STESSA 2009: Behaviour of Steel Structures in Seismic Areas*, Philadelphia, 16-20 aug. 2009, CRC Press 2009, Ed. F.M. Mazzolani, J.M. Ricles, R. Sause, ISBN: 978-0-415-56326-0, 2009.
- [26] Dubina, D., Grecea, D., Stratan, A. & Muntean, N., “Strength and ductility of bolted t-stub macro-components under monotonic and cyclic loading”, *Proc. of SDSS’Rio 2010 Stability and Ductility of Steel Structures*, E. Batista, P. Vellasco, L. de Lima (Eds.), Rio de Janeiro, Brazil, September 8 - 10, 2010.